

y-scaling analysis of the electromagnetic longitudinal and transverse response functions

R. Cenni

Istituto Nazionale Fisica Nucleare, Sezione di Genova, I-16146 Genova, Italy

C. Ciofi degli Atti

*Istituto Nazionale Fisica Nucleare, Sezione Sanità Istituto Superiore di Sanità, Physics Laboratory, I-00161 Rome, Italy
and Department of Physics, University of Perugia, I-06100, Perugia, Italy*

G. Salmè

*Istituto Nazionale Fisica Nucleare,
Sezione Sanità Istituto Superiore di Sanità, Physics Laboratory, I-00161 Rome, Italy
(Received 7 November 1988)*

The electromagnetic longitudinal and transverse inclusive responses for ^{12}C , ^{40}Ca , and ^{56}Fe are analyzed using the concept of y scaling. The longitudinal, F_L , and transverse, F_T , scaling functions are defined, and their experimental values are obtained and compared with the predictions of two theoretical approaches. The first one, based upon the impulse approximation, Hartree-Fock-type wave functions for finite nuclei, and final state interaction treated by complex optical potentials, yields a reasonable interpretation of F_L but cannot predict the experimental splitting between F_L and F_T . The second approach, based on an infinite nuclear matter model, quantitatively reproduces the experimental splitting when the spin and isospin dependence of the effective particle-hole interaction is properly taken into account. The effects of ρ -meson exchange and Δ -hole intermediate states on the scaling functions are also analyzed.

I. INTRODUCTION

In the past few years the Rosenbluth separation of longitudinal (R_L) and transverse (R_T) electromagnetic inclusive response functions for a variety of nuclei,¹⁻⁵ has originated a growing interest in quasielastic (q.e.) scattering, since conventional nuclear models, though being able to explain the total cross section, have shown their inadequacy to simultaneously account for the two response functions; namely, whereas the transverse response can be reasonably reproduced, the longitudinal one is generally overestimated.

In spite of many theoretical efforts for reconciling experiment and theory, based either on some modifications of the properties of nucleons embedded in the nuclear medium (e.g., a sizable modification of their electromagnetic form factors⁶⁻⁸), or on a microscopic description of initial and final nuclear states within realistic treatments of nuclear structure,⁸⁻¹³ a coherent explanation is still waited for.

In order to contribute to the solution of this puzzle we analyze in this paper the role played by some aspects of nuclear dynamics, like e.g., the final state interaction (FSI) and the effective nucleon-nucleon (N - N) interaction in the nuclear medium, in determining the overall features of the longitudinal and transverse responses. To this end, the experimental data will be analyzed in terms of y -scaling, which presents two nontrivial advantages as follows.

(1) The experimental outcomes^{14,15} display a clear scaling property at $y < 0$ (corresponding to energy transfer $\omega < \omega_{\text{peak}}$), while the scaling is badly violated at $y > 0$ (i.e.,

$\omega > \omega_{\text{peak}}$), which corresponds to the kinematical region in which the pion production becomes relevant. Therefore the y -scaling yields a striking signature of the region where the nucleon degrees of freedom are relevant.

(2) The dependence of R_L and R_T upon the momentum transfer for fixed values of y may provide valuable information about those mechanisms which violate the impulse approximation and which may be related to the parameters of the nuclear effective interaction.

In our paper nuclear dynamics will be treated within two different, though complementary, approaches. The first one is based upon a description of q.e. scattering in terms of the distorted wave impulse approximation (DWIA), characterized by initial and final states which are not orthogonal. Such an approach is able to describe surface effects (i.e., the behavior of R_L and R_T at large negative y), but completely fails in accounting for the splitting between the two responses. The second, more microscopic approach is based on Green's function formulation of the many-body problem for infinite nuclear matter. In such a case surface effects cannot be reproduced, but, on the other hand, the splitting between R_L and R_T is not only explained, but is also easily connected with the most relevant features of the particle-hole effective interaction inside the nuclear medium.

Our paper is organized as follows. In Sec. II the general definitions of the longitudinal and transverse scaling functions $F_L(y)$ and $F_T(y)$ will be given. In Sec. III the scaling functions will be analyzed first in plane wave impulse approximation (PWIA) and then taking the FSI into account by means of a complex optical potential. In Sec. IV a more microscopical, state-dependent, FSI will

be introduced through an infinite nuclear matter approach. Finally, in Sec. V our conclusions will be presented.

II. THE LONGITUDINAL AND TRANSVERSE SCALING FUNCTIONS

The cross section for inclusive electron scattering from nuclei, in one photon exchange approximation, is given by (see, e.g., Ref. 16):

$$\begin{aligned} \sigma(q, \omega) &\equiv \frac{d^2\sigma}{d\Omega d\omega} \\ &= \sigma_M \left[\left(\frac{q_\mu^2}{q^2} \right)^2 R_L(q, \omega) \right. \\ &\quad \left. + \left[\frac{1}{2} \frac{q_\mu^2}{q^2} + \tan^2 \frac{\theta}{2} \right] R_T(q, \omega) \right], \end{aligned} \quad (1)$$

where σ_M is the Mott cross section, q and ω the momentum and the energy transfer ($q_\mu^2 = q^2 - \omega^2$), θ the scattering angle and $R_L(q, \omega)$ and $R_T(q, \omega)$ the longitudinal and transverse response functions respectively, which are defined in terms of the electromagnetic current of the nucleus, $J_\mu(q_\mu) \equiv (\mathbf{J}, J_0)$, in the following way:

$$R_L(q, \omega) = \sum_{f \neq i} |\langle \psi_f | J_0 | \psi_i \rangle|^2 \delta(\omega + E_i - E_f), \quad (2)$$

$$R_T(q, \omega) = \sum_{f \neq i} |\langle \psi_f | J_T | \psi_i \rangle|^2 \delta(\omega + E_i - E_f). \quad (3)$$

Here $\psi_i(E_i)$ and $\psi_f(E_f)$ are initial and final eigenstates (eigenvalues) of the A -nucleon Hamiltonian and J_T is the component of the three-vector \mathbf{J} orthogonal to \mathbf{q} . For ease of presentation, nuclear recoil has been neglected in Eqs. (2) and (3). Adding and subtracting the elastic contribution

$$|\langle \psi_i | J_0 | \psi_i \rangle|^2 \delta(\omega),$$

and summing over the final states, it is possible to recast (2) and (3) in the following form¹⁷

$$\begin{aligned} R_L(q, \omega) &= -\frac{1}{\pi} \text{Im} \langle \psi_i | J_0^\dagger \frac{1}{\omega + E_i - H + i\epsilon} J_0 | \psi_i \rangle \\ &\quad - \text{El. cont.}, \end{aligned} \quad (4)$$

$$\begin{aligned} R_T(q, \omega) &= -\frac{1}{\pi} \text{Im} \langle \psi_i | J_T^\dagger \frac{1}{\omega + E_i - H + i\epsilon} J_T | \psi_i \rangle \\ &\quad - \text{El. cont.}, \end{aligned} \quad (5)$$

where H is the Hamiltonian of the nuclear system:

$$H = \sum_{i=1}^A \frac{p_i^2}{2M} + \sum_{i < j} V(i, j). \quad (6)$$

After introducing the corresponding retarded (advanced) total Green function

$$G(E \pm i\epsilon) = \frac{1}{E - H \pm i\epsilon}, \quad (7)$$

Eqs. (4) and (5) can also be expressed through the so-

called polarization propagators $\Pi_{L(T)}(q, \omega)$ (Ref. 17) (it should be pointed out that, since we are only interested in the values $\omega > 0$, the elastic contribution is always vanishing):

$$\begin{aligned} R_{L(T)}(q, \omega) &= -\frac{1}{\pi} \text{Im} \langle \psi_i | J_{0(T)}^\dagger \{ G(\omega + E_i + i\epsilon) \\ &\quad + G(E_i - \omega + i\epsilon) \} J_{0(T)} | \psi_i \rangle \\ &= -\frac{1}{\pi} \text{Im} \Pi_{L(T)}(q, \omega). \end{aligned} \quad (8)$$

Equation (8) is equivalent to Eqs. (4) and (5), since the last term has no imaginary part if $\omega > 0$.

The evaluation of R_L and R_T for a system of nucleons interacting with realistic potentials represents for the time being a prohibitive task, therefore one has to adhere to several approximations which mainly concern the quantities appearing in the rhs of Eqs. (4) and (5), namely (1) the nuclear current, (2) the nuclear wave function, and (3) the total Green's function.

In the usual approach for finite nuclei the nuclear wave function and the total Green's function are treated within distinct approximations, whereas they are handled on the same footing in an approach based on Feynman diagrams expansion for the polarization propagator. Such an approach, however, due to numerical complications, is usually applied to infinite nuclear matter. The approach for finite nuclei will be presented in Sec. III and the nuclear matter approach in Sec. IV. In both cases we are not going to compare, as done by previous works in this field, the experimental and theoretical $R_{L(T)}(q, \omega)$ but rather new quantities which are obtained by analyzing in terms of y scaling the separate responses.

The concept of y scaling has been initially introduced in nuclear physics by West,¹⁸ who has shown that, for a system of nonrelativistic and noninteracting particles, the inclusive cross sections at large momentum transfer can be written as a product of the elementary electron-nucleon cross section, times a nuclear structure function depending only upon the "scaling variable"

$$y_0 = \frac{M}{q} \left[\omega - \frac{q^2}{2M} \right] \quad (9)$$

which represents the longitudinal momentum of a nucleon embedded in a free Fermi gas. Subsequently the concept of y scaling has been generalized to account for relativistic kinematics in the definition of the scaling variable,¹⁴ for nucleon binding and momentum¹⁹ and, finally, for final state interaction.²⁰⁻²² In what follows the theory of Ref. 19 will be adopted. It is based upon the following definition of the *scaling function*

$$F(q, y) = \frac{\sigma(q, y)}{[Z\sigma_{ep} + N\sigma_{en}]} K(q, y), \quad (10)$$

where σ denotes the total inclusive cross section [Eq. (1)], $\sigma_{ep(n)}$ is the electron-proton (neutron) cross section, $K(q, y)$ is a proper phase space factor and $y = y(q, \omega)$ is the *scaling variable* which is defined by the equation giving the energy conservation for q.e. scattering of an elec-

tron off a bound nucleon having minimal values of the momentum and the removal energy. In case of relativistic kinematics this reads

$$\omega + M_A = (M^2 + (y + q)^2)^{1/2} + (M_{A-1}^2 + y^2)^{1/2}, \quad (11)$$

where M_A is the mass of the target and M_{A-1} the mass of the ground state of the $(A-1)$ system. The phase space factor in Eq. (10) is linked to the underlying reaction mechanism which is supposed to occur (see Sec. III).

The importance of γ -scaling analysis in terms of Eq. (10) stems from the observation that if only nucleonic degrees of freedom are considered and the basic reaction mechanism is supposed to be the PWIA, then, at sufficiently high values of q , the scaling function $F(q, y)$ becomes a quantity which depends only upon y (i.e., which "scales" in y) and which represents an integral of the nucleon spectral function. Therefore the analysis of γ scaling in the region where scaling is observed allows one to obtain information on nucleon dynamics, e.g., nucleon momentum distribution, whereas the analysis in the region where scaling is not observed yields information on those effects which break down the impulse approximation.

In view of the available separation between longitudinal and transverse responses it is natural to generalize the concept of γ scaling and to define the following longitudinal and transverse scaling functions (see e.g., Refs. 23 and 24)

$$F_L(q, y) = \frac{R_L(q, y)}{(Z\sigma_{ep}^L + N\sigma_{en}^L)} K(q, y), \quad (12)$$

$$F_T(q, y) = \frac{R_T(q, y)}{(Z\sigma_{ep}^T + N\sigma_{en}^T)} K(q, y), \quad (13)$$

where $\sigma_{ep(n)}^{L(T)}$ is the longitudinal (transverse) contribution of the electron-proton (neutron) cross section appearing in Eq. (10), calculated for a nucleon with energy equal to the minimal removal energy and momentum equal to $|y|$.

It is clear that the separate scaling functions can provide a much richer information on nucleon dynamics than the total one. In the following section the quantities (12) and (13) will be analyzed in PWIA and the effect of FSI will also be illustrated. Since the maximum momentum transfer in the available experimental data on $R_{L(T)}$ is not high enough to give us confidence that the PWIA works and scaling occurs, the main aim of our paper is the investigation of those effects which break the PWIA.

$$R_{L(T)}(q, \omega) = 2\pi \int_{E_{\min}}^{E_{\max}(q, \omega)} dE \int_{k_{\min}(E, q, \omega)}^{k_{\max}(E, q, \omega)} k dk \left| \frac{\partial \omega}{k \partial \cos \alpha} \right|^{-1} \quad (16)$$

(the explicit expression for the relativistic case is given in Ref. 26). The factor $|\partial \omega / k \partial \cos \alpha| = q/M$ originates when integrating over the direction of the initial momentum \mathbf{k} of the ejected nucleon (see Fig. 1). α is the angle between \mathbf{k} and \mathbf{q} , which is fixed, together with k_{\min} , k_{\max} ,

III. FINITE NUCLEI AND THE IMPULSE APPROXIMATION

A. The scaling function within the plane wave impulse approximation

A detailed discussion of the γ -scaling analysis of the inclusive cross section within the framework of the PWIA can be found in Ref. 20 and in Ref. 25 for the nonrelativistic and the relativistic kinematics respectively; the main results of these papers are summarized, generalizing them to the separate response scaling functions. For ease of presentation nonrelativistic kinematics will be used in what follows.

The basic underlying assumptions of the PWIA are as follows.

(1) The electromagnetic current of the nucleus is approximated by the sum of the free nucleon currents

$$J_\mu(q_\mu^2) = \sum_{i=1}^A j_\mu^i(q_\mu^2). \quad (14)$$

(2) Only the direct coupling between virtual photon and emitted nucleon is taken into account (Fig. 1).

(3) The interaction between the emitted nucleon and the residual system is disregarded.

Let us define $|f^{A-1}\rangle, |f'^{A-1}\rangle$ as exact eigenstates of the $(A-1)$ system with eigenvalues E_f^{A-1} and $E_{f'}^{A-1}$. Let also $|\mathbf{p}_f\rangle$ and $|\mathbf{k}_f\rangle$ be plane wave states with momenta \mathbf{p}_f and \mathbf{k}_f describing the A th nucleon which is not correlated with the remaining system; thus, within the PWIA, the matrix element of the total Green function simplifies to:

$$\begin{aligned} & \langle \mathbf{k}_f, f^{A-1} | G(\omega + E_i + i\epsilon) | \mathbf{p}_f, f'^{A-1} \rangle \\ &= \delta(\mathbf{k}_f - \mathbf{p}_f) \delta(E_f^{A-1} - E_{f'}^{A-1}) \\ & \times \frac{1}{\omega + E_i - (E_f^{A-1} + T_{A-1} + k_f^2/2M) + i\epsilon}, \end{aligned} \quad (15)$$

where T_{A-1} is the kinetic energy of the center of mass of the residual system. Therefore, summing over the final states of the ejected nucleon and of the remaining $(A-1)$ system, one obtains (for ease of presentation the spin-isospin variables are omitted):

$$[ZP_p(k, E)\sigma_{L(T)}^p + NP_n(k, E)\sigma_{L(T)}^n], \quad (16)$$

and E_{\max} , by the energy conservation

$$\omega = \frac{(\mathbf{k} + \mathbf{q})^2}{2M} + \frac{k^2}{2M_{A-1}} + E \quad (17)$$

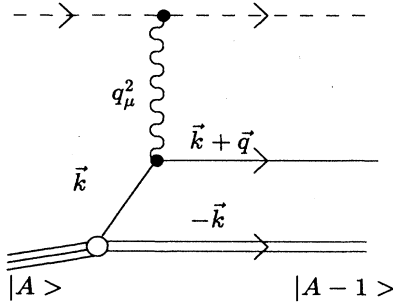


FIG. 1. Diagram describing the direct interaction between the virtual photon and the emitted nucleon.

and eventually $E_{\min} = M_{A-1} + M - M_A$. In Eq. (16)

$$P_p(k, E) = \sum_{f^{A-1}} |\langle \mathbf{k}, f^{A-1} | \psi_i \rangle|^2 \delta(E + E_i - E_f^{A-1}) \quad (18)$$

is the spectral function, which yields the probability distribution of finding in the target nucleus a nucleon with momentum $k = |\mathbf{k}_f - \mathbf{q}|$ and removal energy $E = E_f^{A-1} - E_i$.

Disregarding in R_T the convection current, which gives a contribution of the order of few percent, one obtains

$$R_L(q, \omega) = [ZG_E^{p2}(q_\mu^2) + NG_E^{n2}(q_\mu^2)] \times \left[1 - \frac{q^2}{4M^2} \right] \left| \frac{\partial \omega}{k \partial \cos \alpha} \right|^{-1} I(q, \omega), \quad (19)$$

$$R_T(q, \omega) = [ZG_M^{p2}(q_\mu^2) + NG_M^{n2}(q_\mu^2)] \frac{q^2}{2M^2} \left| \frac{\partial \omega}{k \partial \cos \alpha} \right|^{-1} I(q, \omega), \quad (20)$$

where $G_E^{p(n)}$ and $G_M^{p(n)}$ are the electric and magnetic Sachs form factors, respectively, and $I(q, \omega)$ is the nuclear structure function given by

$$I(q, \omega) = 2\pi \int_{E_{\min}}^{E_{\max}(q, \omega)} dE \int_{k_{\min}(E, q, \omega)}^{k_{\max}(E, q, \omega)} k dk P(k, E) \quad (21)$$

(the equality between proton and neutron spectral functions has been assumed, i.e., $P_p = P_n$). Let us introduce the nonrelativistic analogue of Eq. (11), i.e., the energy conservation for a nucleon with momentum $k = |y|$ and removal energy $E = E_{\min}$

$$\omega - E_{\min} = \frac{(y + q)^2}{2M} + \frac{y^2}{2M_{A-1}}. \quad (22)$$

The longitudinal and transverse responses can then be expressed in terms of q and y instead of q and ω . If the PWIA is assumed to hold, the general criterion for defining the scaling function is that it should represent the nuclear structure function; therefore the following definitions will be adopted in what follows:

$$F_L^{th}(q, y) = \frac{R_L(q, y)}{[ZG_E^{p2}(q_\mu^2) + NG_E^{n2}(q_\mu^2)](1 - q^2/4M^2)} \times \left| \frac{\partial \omega}{k \partial \cos \alpha} \right|, \quad (23)$$

$$F_T^{th}(q, y) = \frac{R_T(q, y)}{[ZG_M^{p2}(q_\mu^2) + NG_M^{n2}(q_\mu^2)]q^2/2M^2} \left| \frac{\partial \omega}{k \partial \cos \alpha} \right|, \quad (24)$$

which have the same general form as Eqs. (12) and (13), with $K(q, y) = |\partial \omega / k \partial \cos \alpha| = q/M$. Placing (19) and (20) in (23) and (24) one obtains $F_L = F_T = I(q, y)$. In order to check such a strong prediction from the PWIA we have constructed the experimental longitudinal and transverse scaling functions, F_L^{exp} and F_T^{exp} , for ^{12}C , ^{40}Ca , and ^{56}Fe using in the numerators of Eqs. (12) and (13) the results of Refs. 3 and 4. The phase space factor $K(q, y)$ and the cross sections $\sigma_{\text{ep}(n)}^{L(T)}$ which appear in the denominators have been calculated using fully relativistic kinematics (in particular the relativistic electron-nucleon cross section cc^1 of Ref. 27 and the nucleon form factor of Ref. 28 have been adopted). The results are presented in Figs. 2, 3, and 4. It can be seen that F_L^{exp} and F_T^{exp} are different in the whole range of momentum transfer considered; moreover they decrease for large values of y and seem to slowly approach a scaling behavior. Since the experimental data cover a small kinematical region at low momentum transfer, these results are not very sensitive to the choice of $\sigma_{\text{ep}(n)}$, the nucleon form factors and the kinematics (the order of magnitude of the uncertainties produced by alternative choices amount to 15%, at most). Therefore the scaling properties of F_L^{exp} and F_T^{exp} will be analyzed in the following using nonrelativistic kinematics.

The experimental splitting between F_L^{exp} and F_T^{exp} is in sharp contrast with the prediction of the PWIA represented by the dotted lines in Figs. 2, 3, and 4 which have been obtained using a Hartree-Fock-type function for initial and residual systems, i.e.,

$$P(k, E) = \sum_{\alpha \in \{\text{occupied states}\}} |\phi_\alpha(k)|^2 \delta(E + \epsilon_\alpha), \quad (25)$$

where ϕ_α is the Fourier transform of the single particle wave function and ϵ_α is the proper eigenvalue; one gets for the scaling function

$$I(q, y) = 2\pi \sum_\alpha \int_{k_{\min}(q, y, \epsilon_\alpha)}^{k_{\max}(q, y, \epsilon_\alpha)} |\phi_\alpha(k)|^2 k dk. \quad (26)$$

It can be seen that at the q.e. peak (corresponding to $y=0$) the longitudinal response is strongly overestimated. We reiterate, however, that the main inadequacy of the PWIA is its inability to split F_L and F_T .

B. The distorted wave impulse approximation

The first correction to the PWIA which has to be considered is the FSI between the emitted nucleon and the

$$\langle \mathbf{k}_f, f^{A-1} | G(\omega + E_i + i\epsilon) | \mathbf{p}_f, f'^{A-1} \rangle$$

$$= \delta(\mathbf{k}_f - \mathbf{p}_f) \delta(E_f^{A-1} - E_f^{A-1}) \frac{\mathcal{P}(E_N)}{\omega + E_i - (E_f^{A-1} + T_{A-1} + k_f^2/2M + V(E_N)) + iW(E_N)}, \quad (27)$$

where E_N is the final energy of the nucleon in the centre of mass of the A system:

$$E_N = \omega + E_i - E_f^{A-1} - T_A, \quad (28)$$

residual system, which has been introduced in our scheme by modifying the matrix element of the total Green's function, Eq. (7). Actually we used a single particle Green's function with a complex energy-dependent potential, that describes the interaction between the nucleon and the residual system, obtaining instead of Eq. (15) the following expression:

$\mathcal{P}(E_N)$ is the Perey factor

$$\mathcal{P}(E_N) = 1 - \frac{\partial V(E_N)}{\partial E_N}, \quad (29)$$

and $V(E_N)$ (Ref. 29) and $W(E_N)$ (Ref. 30) are the real and imaginary parts of the optical potential, given by:

$$V(E_N) = -[E + \frac{1}{2}(2n + l + \frac{3}{2})\omega_{\text{osc}}] \exp[-(E_N + E)/E_0], \quad (30)$$

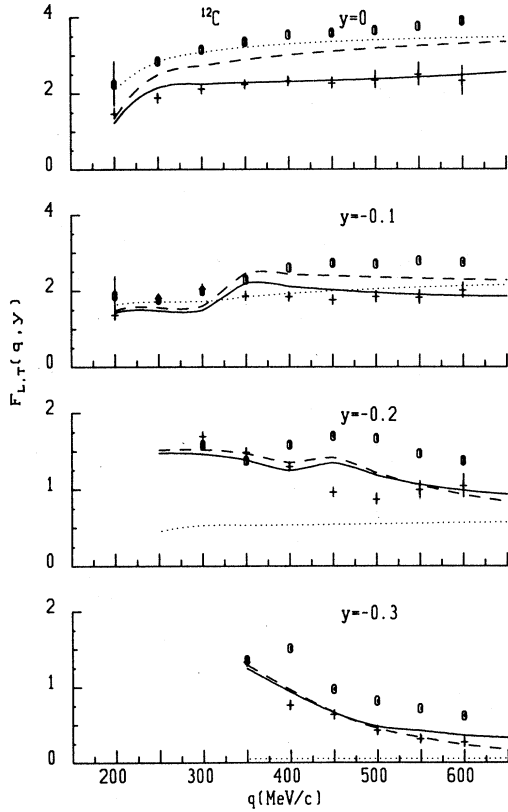


FIG. 2. Longitudinal and transverse scaling functions for ^{12}C vs the momentum transfer q for several values of the scaling variable y defined by Eq. (11). Crosses and open circles denote, respectively, F_L and F_T obtained from Eqs. (12) and (13) using for $R_{L(T)}$ the experimental data from Ref. 3 and for $\sigma_{\text{ep}(n)}^{L(T)}$ the relativistic off-shell cross section from Ref. 27. Dotted lines represent the PWIA results, dashed lines the DWIA with real potential, and solid lines the DWIA with complex optical potential. In this and in following figures scaling functions and variables are expressed in units of the nucleon mass.

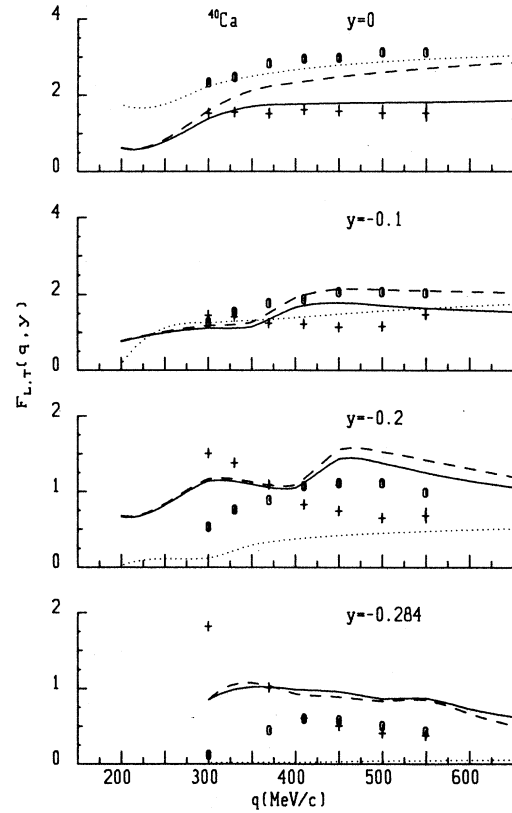


FIG. 3. The same as Fig. 2 but for ^{40}Ca . Experimental data for $R_{L(T)}$ from Ref. 4.

$$W(E_N) = C(E_N + E)^2 \exp(-(E_N + E)/E_0), \quad (31)$$

with $E_0 = 4k_f^2/2M$ and $C = -4.5 \times 10^{-3} \text{ MeV}^{-1}$.

The dynamics included in this parametrization of the Green's function is in principle quite rich, but, as we shall see, it is nevertheless not sufficient to explain the

differences between the longitudinal and transverse channels [the microscopical meaning of (27) will be discussed in more details in the next section].

Equation (27) leads to the following expression for $F_{L(T)}$:

$$F_{L(T)}(q, y) = -\frac{1}{\pi} \int_{E_{\min}}^{\infty} dE \int d^3k \frac{P(E_N)W(E_N)P(k, E)}{\{\omega + E_i - [E_f^A - 1 + T_{A-1} + (\mathbf{k} + \mathbf{q})^2/2M + V(E_N)]\}^2 + W(E_N)^2}. \quad (32)$$

Due to the fact that, for fixed y , E_N increases with q , also V and W decrease, and therefore the asymptotic value of $F_{L(T)}$ is the same as in the case of the pure PWIA. In Figs. 2, 3, and 4 the theoretical results obtained using Eq. (32) are presented by the full curves (the dashed curves represent the results obtained from a purely real optical potential); it can be seen that the q -behavior of the longitudinal scaling function is qualitatively reproduced, at least near the top of the peak, displaying, at low q , some structure due to the effects of the shells, but no splitting between F_L and F_T is obtained. It is clear that in order to obtain such a splitting further

improvements in the evaluation of the matrix element of the e.m. current of the nucleus would be necessary. As a matter of fact, we have considered only the direct term (Fig. 1) in the e.m. coupling of the electron with the nucleus, but the antisymmetrization, or recoil, term could be relevant. If these terms are taken into account the inclusive cross section does no longer factorize and moreover different final states of the residual system are generated, due to the different structure of J_0 and J_T in the spin-isospin subspace. This fact has important consequences, in that the FSI acting differently in the longitudinal and transverse channels is now able to distinguish the two responses. Such a mechanism will be illustrated in the following section within a simple but significant model.

IV. INFINITE NUCLEAR MATTER MODEL

We have seen in the previous section that by introducing the FSI it is possible to qualitatively explain the longitudinal response but no splitting between F_L and F_T can be obtained.

In order to understand this phenomenon let us remember the connection between Eqs. (2) and (3) and Eqs. (4) and (5): In the latter, the final states $|\psi_f\rangle$ represent the intermediate states of the propagation of the system. We may for instance consider intermediate particle-hole states only. If we assume that both the particle and the hole interact with the surrounding medium (i.e., they move under the effect of an optical potential) but not between themselves, then no splitting between longitudinal and transverse channels arises. This is the case, *a fortiori*, of the PWIA, when the ejected nucleon evolves under the action of the free Hamiltonian; the same happens in the DWIA as far as the exact Green's function of the system is approximated by a single particle Green's function, since in this way it cannot carry information on the state of the residual system, apart from the missing energy and momentum. If we assume, on the contrary, that some interaction between the particle and the hole occurs, then in principle this interaction will depend upon the quantum numbers of the particle-hole pair and, consequently, it may distinguish between different channels.

To improve our understanding of many of the features described above, and in particular shed some more light on the role of and on the precise meaning of the final state interactions, we wish to examine here a simple ap-

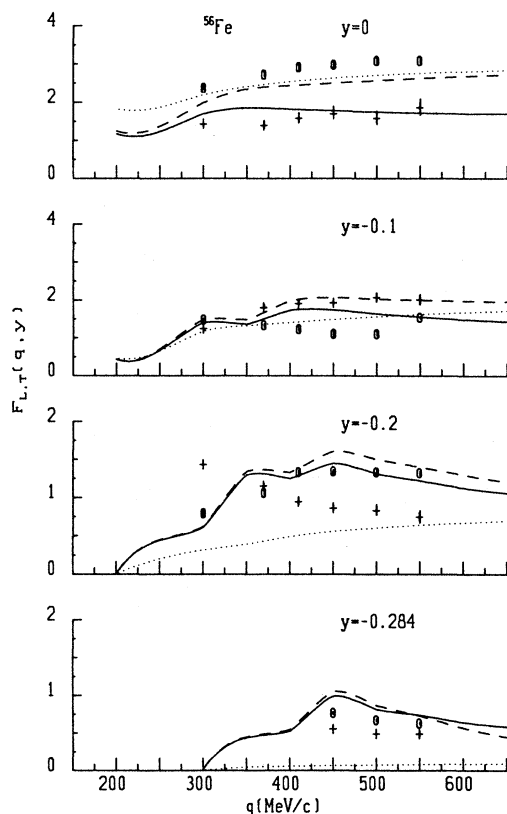


FIG. 4. The same as Fig. 2 but for ^{56}Fe . Experimental data for $R_{L(T)}$ from Ref. 4.

proach based on infinite nuclear matter. Something will be lost of course, since in this frame surface effects are forcibly ignored, which may be relevant at high values of γ but we gain in improving our understanding of the details of the process.

Moreover, we may understand in this frame why the γ -scaling hypothesis holds in simple cases and why it is violated in more sophisticated approaches. In order to follow step by step the physical origin of the deviations from the γ -scaling hypothesis we start from the lowest possible level of complication, namely the free Fermi gas model, and then we shall introduce other effects one at a time.

A. The Fermi gas model

The response of a system to an external probe which couples to the nuclear density is expressed through the polarization propagator $\Pi_L(q, \omega)$ [cf., Eq. (8)]. In the free Fermi gas model, where no interaction is present, $\Pi_L(q, \omega)$ simply reduces (up to electromagnetic form factors or trivial coefficients) to the Lindhard function, which reads¹⁷

$$\Pi^0(q, \omega) = \int \frac{d^3k}{(2\pi)^3} \theta(|\mathbf{q} + \mathbf{k}| - k_F) \theta(k_F - k) \times \left\{ \frac{1}{\omega - \frac{q^2}{2M} - \frac{\mathbf{q} \cdot \mathbf{k}}{M} + i\eta} - \frac{1}{\omega + \frac{q^2}{2M} + \frac{\mathbf{q} \cdot \mathbf{k}}{M} - i\eta} \right\}. \quad (33)$$

$$\Pi^{\text{HF}} = \int \frac{d^3k}{(2\pi)^3} \theta(|\mathbf{q} + \mathbf{k}| - k_F) \theta(k_F - k) \frac{1}{\omega - \frac{q^2}{2M} - \frac{\mathbf{q} \cdot \mathbf{k}}{M} - \Sigma(|\mathbf{q} + \mathbf{k}|) + \Sigma(k) + i\eta} + \text{advanced term}. \quad (36)$$

Since our attitude will be that of parametrizing Σ , we may of course imagine to parametrize the exact self-energy. The system we are describing in the frame of Eq. (36) corresponds to a particle-hole excitation, with the particle (and the hole) interacting with the surrounding medium. In other words this corresponds to a knock-out process in which the ejected nucleon propagates under the effect of the optical potential of the spectator system; the latter can be not only in the ground state but, in general, in an excited state, with a dressed hole left by the ejected nucleon propagating in it. We neglect however any interaction between the ejected nucleon and the hole left in the residual system. In other words, apart from the more or less suitable parametrizations, we are describing the same kind of physical situation of the DWIA. We remind once more that no difference may

The longitudinal and transverse scaling functions (12) and (13) can be easily found by considering that the Feynman diagram expansions for Π_L and Π_T , as defined in Eq. (8), are topologically coincident, the only differences being in the initial and final vertices. One gets for the free Fermi gas scaling function $F_{L(T)}^{\text{FG}}$:

$$F_{L(T)}^{\text{FG}} = -\frac{1}{\pi} \frac{q}{M} \frac{2}{\rho} \text{Im} \Pi^0(\mathbf{q}, \omega) \quad (34)$$

(ρ being the nuclear density). One immediately recognizes that for $\omega > 0$ only the retarded term contributes to the imaginary part. If moreover the kinematical region $q > 2k_F$ is considered, F^{FG} can be rewritten as

$$F^{\text{FG}} = -\frac{1}{\pi} \frac{q}{M} \frac{2}{\rho} \text{Im} \int \frac{d^3k}{(2\pi)^3} \frac{\theta(k_F - k)}{\omega - \frac{q^2}{2M} - \frac{\mathbf{q} \cdot \mathbf{k}}{M} + i\eta} = -\frac{1}{\pi} \frac{1}{M} \frac{2}{\rho} \text{Im} \int \frac{d^3k}{(2\pi)^3} \frac{\theta(k_F - k)}{\frac{y_0}{M} - \frac{k \cos \alpha}{M} + i\eta}. \quad (35)$$

Equation (35) shows that $F_{L(T)}$ depends on q and ω through the West's scaling variable y_0 defined by (9), i.e., the original result of West is recovered.

B. The Hartree-Fock approximation

The next level of complication is to assume that nucleons move in a mean field (Hartree-Fock approximation), which amounts to add a self-energy in the denominators of Eq. (33); one has in this frame

arise in this case between longitudinal and transverse channels because only the internal propagation of nucleons has been changed, which does not depend upon the initial and final vertices.

To further simplify the problem let us assume a very elementary model for the self-energy

$$\frac{k^2}{2M} + \Sigma(k) \simeq \begin{cases} \frac{k^2}{2M^*} - A, & \text{if } k < k_F; \\ \frac{k^2}{2M} + B, & \text{if } k > k_F. \end{cases} \quad (37)$$

Using the preceding definitions one easily finds

$$F_{L(T)}^{\text{HF}}(y_0, q) = -\frac{1}{\pi} \frac{1}{M} \frac{2}{\rho} \text{Im} \int \frac{d^3k}{(2\pi)^3} \theta(k_F - k) \frac{1}{\frac{y_0}{M} - \frac{k \cos \alpha}{M} - \left[\frac{k^2}{2M} - \frac{k^2}{2M^*} + A + B \right] / q + i\eta} \quad (38)$$

It can be seen that this new quantity depends both on q and y_0 . However the q dependence which breaks the scaling property has two contributions: The first one, namely $(k^2/2M - k^2/2M^*)/q$ is clearly weak in the spirit of the hole-line expansion, since it leads to higher powers of k_F . The second one, which is instead relevant, comes from the different potential energies felt by the nucleon inside and outside the nuclear medium (here it coincides just with the quantity $\bar{\epsilon} = A + B$). However this object does not depend on the integration variable, so that a change in the definition of the scaling variable is naturally suggested. Let us define

$$y_{\text{HF}} = \frac{M}{q} \left[(\omega - \bar{\epsilon}) - \frac{q^2}{2M} \right]. \quad (39)$$

We find

$$F^{\text{HF}}(y_{\text{HF}}, q) = -\frac{1}{M} \text{Im} \int \frac{d^3k}{(2\pi)^3} \theta(k_F - k) \frac{1}{\frac{y_{\text{HF}}}{M} - \frac{k \cos \alpha}{M} - \left[\frac{k^2}{2M} - \frac{k^2}{2M^*} \right] / q + i\eta} \quad (40)$$

Of course the new definition of the scaling variable depends on the assumptions on Σ done in Eq. (37). The evaluation of Eq. (40) is an easy task and an explicit calculation at y_{HF} fixed, shows indeed an extremely low dependence on q .

The physical insight which comes out from these elementary considerations is that within a Green's function many-body approach the choice of the scaling variable and consequently the scaling properties of the scaling function depends upon the explicit form of the self-energy. It can be seen from Eq. (40) that, in disagreement with experimental observations, no splitting between F_L and F_T is predicted by the HF approximation.

The weakness of the Hartree-Fock approximation is the lack of the imaginary part of the self-energy, which is connected with complicated many-body intermediate states like 2 (or more) particles-2 (or more) holes,³¹ and will be discussed at the end of this section.

A further drawback comes from the neglecting of any residuum at the pole, or in other words from the momentum distribution which in our formulas is that of the free Fermi gas. As a consequence at high values of y the HF approximation goes wrong, while the DWIA described in Sec. III, being a much more sophisticated parametrization, did provide better agreement with the data in that region. In the following subsections the scaling functions (23) and (24) will be plotted versus the scaling variable corresponding to the HF approximation and, by considering various improvements of the latter, we will try to understand the physical origin of the splitting between F_L and F_T .

C. The residual interaction

The correction to the HF approximation which will be now considered is the effective p - h interaction, which, to begin with, is assumed to be constant and independent from the quantum numbers of the p - h pair. Let us

denote it by V_0 . The Bethe-Salpeter equation for the full polarization propagator becomes algebraic (in practice the RPA series) and one gets

$$\Pi^{\text{tot}}(q, \omega) = \frac{\Pi^{\text{HF}}(q, \omega)}{[1 - V_0 \Pi^{\text{HF}}(q, \omega)]} \quad (41)$$

The physical effects introduced here are often referred to in the literature³² as rescattering corrections. From a many-body point of view however these corrections come about by antisymmetrizing the interaction between the ejected nucleon and the remaining hole in the residual system. In this sense they could be described as final state interaction too. This is an important improvement with respect to the HF approximation, which brings about the central problem of our paper, namely whether the FSI can be considered the origin of the splitting between F_L and F_T .

For sake of simplicity we ignore for the moment the structure of the vertices (to be discussed later) and assume the interaction to be channel-independent. The scaling function is, explicitly writing the imaginary part,

$$F_{L(T)}^{\text{tot}} = \frac{F^{\text{HF}}}{(1 - V_0 \text{Re} \Pi^{\text{HF}}(q, \omega))^2 + (\pi \rho V_0 F^{\text{HF}} M / 2q)^2} \quad (42)$$

This equation shows that no splitting between F_L and F_T can be obtained within a constant channel independent p - h interaction and that the scaling property is violated for two reasons. The first one is the existence in the denominator of the term $(\pi \rho M V_0 F^{\text{HF}})^2 / 4q^2$, which clearly depends on q , and which is vanishing small as $q \rightarrow \infty$. The second point is the dependence of F^{tot} on $\text{Re} \Pi^{\text{HF}}$. Let us remember that $\text{Re} \Pi^{\text{HF}}$ has a retarded and an advanced part. The functional dependence of the first one is like $\varphi(y_{\text{HF}})/q$ and is vanishing for $y_{\text{HF}} = 0$ (this statement is for instance trivial for the Lindhard function Π_0). The advanced part instead is given, in the low densi-

ty limit, by

$$\Pi_{\text{adv}}^{\text{HF}} \simeq - \frac{\rho}{\omega + \frac{q^2}{2M} + \bar{\epsilon}}. \quad (43)$$

This clearly shows the breaking down of the scaling property and again shows that these effects disappear at higher values of q . A new physical effect is taken into account here since the advanced part of the Lindhard function may introduce into the game initial state correlations as well: In fact if one translates the Feynman diagram language into the old-fashioned (Brückner) perturbation theory, one sees that the advanced part of $\text{Re}\Pi^{\text{HF}}$ makes it possible 2p-2h (or more) excitations to occur before the photon is absorbed, which just describe corrections to the single-particle wave function of the initial state.³³

We remind that the experimental data presented before concern transferred momenta up to 600 MeV/c which are not yet in the asymptotic region. From our discussion we may argue in which direction the scaling property is broken. It is clear in fact that the term $(\pi\rho MV_0 F^{\text{HF}})^2/4q^2$ entails always a depletion of the quasielastic peak. The other term has quite a clear behavior at $y_{\text{HF}}=0$ since it reduces to $(1-V_0\text{Re}\Pi_{\text{adv}}^{\text{HF}})^2$, and Eq. (43) shows that $\text{Re}\Pi_{\text{adv}}^{\text{HF}}$ is negative. It follows that a repulsive effective interaction leads to a term >1 which cooperates with the previous term to reduce the scaling function F^{tot} . Since the asymptotic value is F^{HF} , then F^{tot} reaches this value from below. The case of attractive interaction is more involved since the two contributions have opposite effects and only a strongly attractive interaction shall give an enhancement of F^{tot} .

Let us eventually consider the case of a realistic p - h interaction, namely the one which is obtained in the frame of the Landau-Migdal theory. The usual Ansatz is

$$V^{p-h} = C_0[\mathcal{F}_0 + \mathcal{F}'_0\tau_1\cdot\tau_2 + \mathcal{G}_0\sigma_1\cdot\sigma_2 + \mathcal{G}'_0\tau_1\cdot\tau_2\sigma_1\cdot\sigma_2], \quad (44)$$

with

$$C_0 = \frac{2\pi^2}{k_F M^*(k_F)}. \quad (45)$$

The apparent dependence of the effective interaction on the particular spin-isospin channel has an immediate consequence: In fact a longitudinal interaction propagates only in the $S=0$ channel, while a transverse one propagates in the $S=1$ channel, so that different Landau parameters are involved. In this way the degeneracy of F_L and F_T is necessarily broken.

Since the longitudinal vertex is $\frac{1}{2}[1+\tau_3]$, a little bit of algebra provides for Π_L the expression

$$\Pi_L = \frac{1}{2} \frac{\Pi^{\text{HF}}}{1-C_0\mathcal{F}_0\Pi^{\text{HF}}} + \frac{1}{2} \frac{\Pi^{\text{HF}}}{1-C_0\mathcal{F}'_0\Pi^{\text{HF}}} \quad (46)$$

[Eq. (41) is regained when the interaction in the isoscalar and isovector channels coincide].

For Π_T , if convection current is neglected, the following expression can be easily obtained:

$$\begin{aligned} \Pi_T &= \frac{(\mu_p + \mu_n)^2}{2(\mu_p^2 + \mu_n^2)} \\ &\times \frac{\Pi^{\text{HF}}}{1-C_0\mathcal{G}_0\Pi^{\text{HF}}} + \frac{(\mu_p + \mu_n)^2}{2(\mu_p^2 - \mu_n^2)} \frac{\Pi^{\text{HF}}}{1-C_0\mathcal{G}'_0\Pi^{\text{HF}}}. \end{aligned} \quad (47)$$

The parametrization for the transverse response, given by Eq. (47), does not contain several effects whose relevance should be carefully investigated. To this end, let us note first of all that numerically the weights for the isoscalar and isovector channels are respectively 0.03 and 0.97, so that considering propagation through the isovector channel only, viz.

$$\Pi_T \simeq \frac{\Pi^{\text{HF}}}{1-C_0\mathcal{G}'_0\Pi^{\text{HF}}} \quad (48)$$

appears to be an excellent approximation.

This channel, unlike the longitudinal one, cannot be fully described in a conventional approach based on more or less realistic N - N potentials but requires an explicit treatment of ρ -meson exchange and intermediate isobar configurations. The effective interaction in this channel is therefore usually written as ($f^2/4\pi=0.08$)

$$V^{11} = \frac{f^2}{m_\pi^2} \left[g' + C_\rho \frac{q^2}{\omega^2 - q^2 - m_\rho^2} \right], \quad (49)$$

with $C_\rho=2.3$ (Ref. 34) and where the parameter g' is connected to \mathcal{G}'_0 by

$$C_0\mathcal{G}'_0 = \frac{f^2}{m_\pi^2} g'. \quad (50)$$

Moreover in this channel the Δ - h intermediate states are allowed and provide the following contribution to the transverse polarization propagator: If we introduce the Δ - h propagator as

$$\Pi^{\Delta-h}(q, \omega) = \phi(q, \omega) + \phi(q, -\omega), \quad (51)$$

$$\phi(q, \omega) = \frac{16}{9} \int \frac{d^3k}{(2\pi)^3} \frac{\theta(k_F - k)}{\omega - M_\Delta + M - \frac{(\mathbf{q} + \mathbf{k})^2}{2M_\Delta} + \frac{k^2}{2M} + i\eta}, \quad (52)$$

the whole polarization propagator then is obtained by means of the replacement

$$\Pi^{\text{HF}} \rightarrow \Pi^{\text{HF}} + \frac{f_{\pi N\Delta}^2}{f^2} \Pi^{\Delta-h} \quad (53)$$

in Eq. (48). In the following, as usual, we put $f_{\pi N\Delta}=2f$.

In Fig. 5 the scaling functions of ^{40}Ca calculated for two different values of y are presented. The results deserve several comments as follows.

(1) The splitting between the two responses due to the particle-hole interaction is demonstrated.

(2) A repulsive p - h interaction is necessary in order to obtain a quenching of the longitudinal scaling function with respect to the HF results.

(3) The relevant contribution of the ρ -meson exchange is clearly put in evidence.

(4) The effect of Δ - h intermediate states is also relevant at the top of the q.e. peak ($y=0$) while it becomes negligible for high negative values of the scaling variable.

Having established the important role played by the effects due to ρ -meson exchange and to the Δ - h intermediate states, a systematic calculation of F_L and F_T for ^{12}C , ^{40}Ca , and ^{56}Fe has been performed, taking these effects into account. Following Moniz³⁵ the Hartree-Fock parameters are $\bar{\epsilon}=20$ MeV, 30 MeV, 40 MeV, and $k_F=220$ MeV/c, 230 MeV/c, 240 MeV/c for ^{12}C , ^{40}Ca , and ^{56}Fe , respectively. The results, which are presented in Figs. 6, 7, and 8, clearly show that, for all nuclei considered, the splitting between the longitudinal and transverse scaling functions can systematically be obtained with a unique set of parameters for the p - h interaction, ρ -meson exchange and Δ - h intermediate states. It can

also be seen that the depletion of the longitudinal channel requires a repulsive effective interaction, while the experimental data in the transverse one suggest a weak attraction.

Let us now discuss the sensitivity of our results upon the choice of the Landau parameters; this is a really crucial problem since for these quantities many estimates are available. As to the longitudinal channel for instance, Speth *et al.*³⁶ found, from the analysis of the low-lying states of lead, values compatible with $\mathcal{F}_0 \approx 0$ and $\mathcal{F}'_0 \approx 0.65$, which implies on the whole a repulsive interaction.

Another evaluation for these coefficients is hidden in the parameters of the Skyrme forces, since in practice in the particle-hole channel they simply correspond to a Landau-Migdal effective interaction [like in Eq. (44)] with in addition a p -wave interaction. A translation from

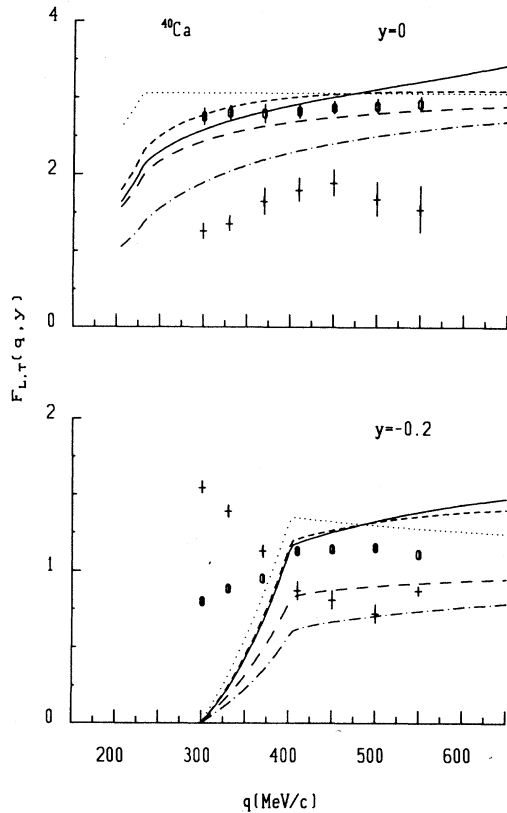


FIG. 5. Longitudinal and transverse scaling functions for ^{40}Ca vs the momentum transfer q for two values of the scaling variables defined by Eq. (39). Crosses and open circles denote, respectively, F_L and F_T obtained from Eqs. (12) and (13) using for $R_{L(T)}$ the experimental data from Ref. 4 but for $\sigma_{ep(n)}^{L(T)}$ the nonrelativistic cross section. Dotted lines denote the pure Hartree-Fock response. Including the particle-hole interaction with $\mathcal{F}_0=\mathcal{F}'_0=1$ and $g'=0.5$ leads to the splitting of the responses represented by the dot-dashed (F_L) and long-dashed (F_T) lines. The short-dashed lines include the effect of the ρ -meson exchange and the solid lines also the contribution of the Δ - h intermediate states. Here $C_\rho=2.3$, $k_F=230$ MeV, $\bar{\epsilon}=30$ MeV, $M^*=0.7M$. In evaluating C_0 [Eq. (45)] the value $M^*(k_F)=M$ is used.

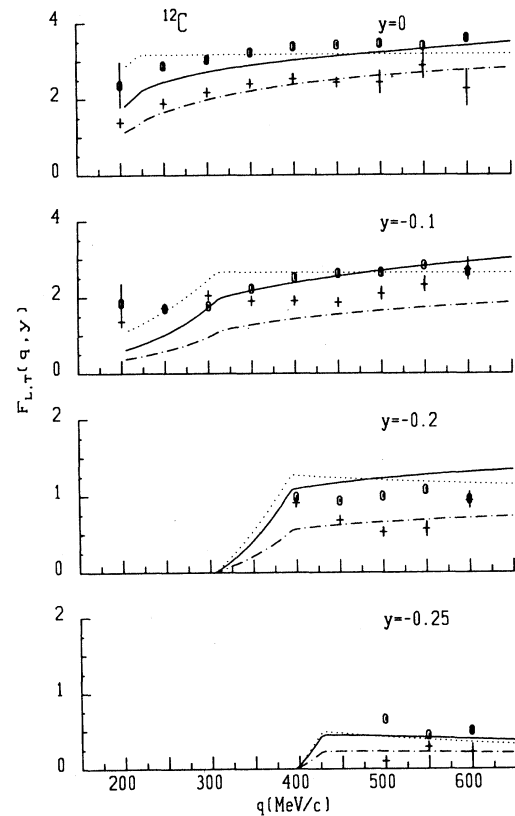


FIG. 6. Longitudinal and transverse scaling functions for ^{12}C vs the momentum transfer q for several values of the scaling variable y_{HF} defined by Eq. (39). Crosses and open circles, denote respectively, F_L and F_T obtained from Eqs. (12) and (13) using for $R_{L(T)}$ the experimental data from Ref. 3 and for $\sigma_{ep(n)}^{L(T)}$ the nonrelativistic cross section. The dash-dotted lines represent the longitudinal response, the solid lines the transverse one, and the dotted lines denote the pure Hartree-Fock result. Parameters for the p - h interaction [Eq. (44)], ρ -exchange [Eq. (49)], and Δ - h [Eqs. (51) and (52)] contributions as in Fig. 5.

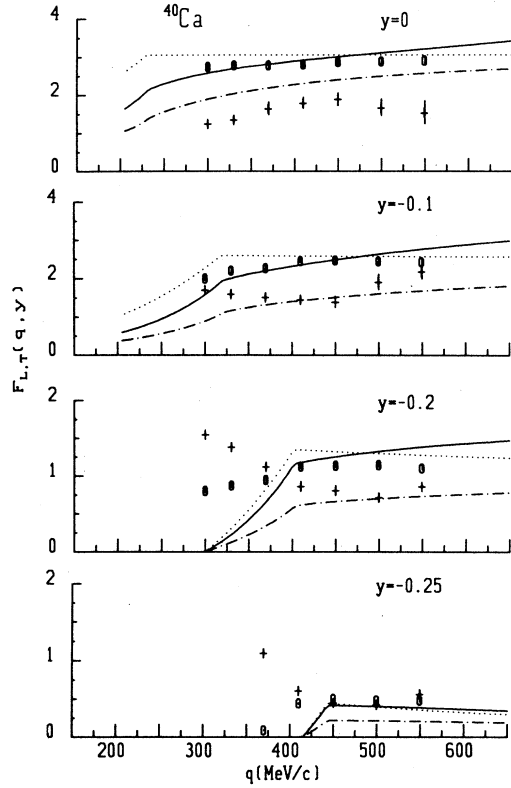


FIG. 7. The same as in Fig. 6 but for ^{40}Ca . Experimental data for $R_{L(T)}$ from Ref. 4.

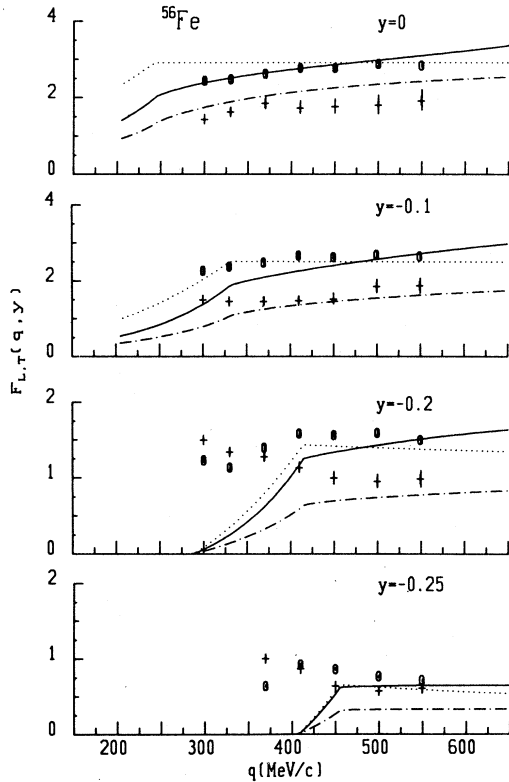


FIG. 8. The same as in Fig. 6 but for ^{56}Fe . Experimental data for $R_{L(T)}$ from Ref. 4.

particle-particle to particle-hole parameters for Skyrme forces is found in Ref. 37. The various kinds of forces give a quite uncertain value for \mathcal{F}_0 (ranging between -0.45 to 0.74) and a \mathcal{F}'_0 which at least is always repulsive. In particular the Skyrme III interaction, which has been used in Ref. 10, provides $\mathcal{F}_0 \approx 0.3$ and $\mathcal{F}'_0 \approx 0.87$; it is clear from our previous analysis that a RPA calculation with this repulsive interaction should provide a lowering of the quasielastic peak, as it was indeed found in Ref. 10.

A very strong repulsion is obtained if, as in Ref. 8, the relations between \mathcal{F}_0 , \mathcal{F}'_0 , the nuclear compressibility and the asymmetry coefficient of the mass formula are used: with these expressions one finds (with $m^* = m$) $\mathcal{F}_0 = 1.89$ and $\mathcal{F}'_0 = 4.06$. Such a repulsion could be lowered by introducing a cutoff function which produces a strong decrease of the repulsion with increasing q . This procedure is quite reasonable since the assumption that the Landau parameters are independent on the energy and momentum transfers is surely questionable, but at present there are no insights on what kind of q dependence one should require. In Ref. 8 the cutoff function has been fixed by fitting the longitudinal response function.

In Fig. 9 the sensitivity of F_L upon the Landau-Migdal parameters \mathcal{F}_0 and \mathcal{F}'_0 is illustrated for ^{40}Ca : It appears that the effect of the variation of the parameters is of

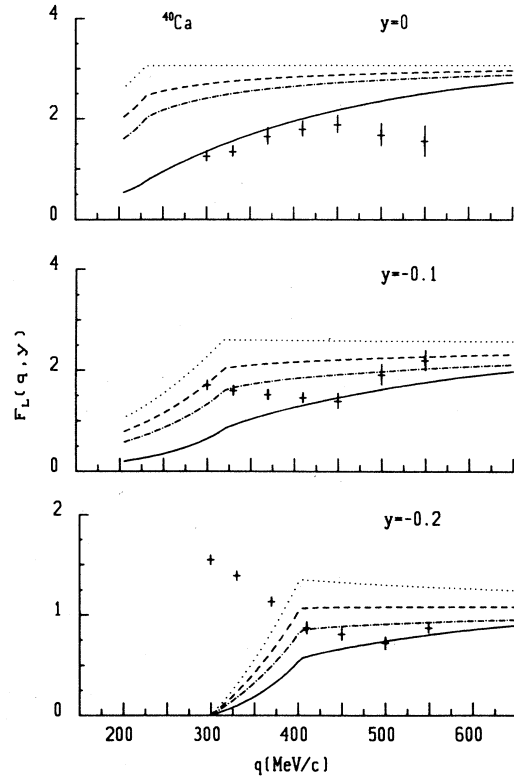


FIG. 9. Longitudinal scaling function for ^{40}Ca for different effective interactions. Scaling variable and experimental data as in Fig. 7. Dashed lines correspond to the parameters of Ref. 36, dash-dotted lines correspond to the parameters of Skyrme III interaction, solid lines to the parameters of Ref. 8. The dotted lines represent pure Hartree-Fock approximation.

minor relevance at high q , where all curves, corresponding to different sets of parameters, approach the HF result. The best agreement with experimental data is achieved by using the values of Ref. 8, and at $y=0$ it is indeed very good, without any change of the free nucleon form factor as advocated in Ref. 8. There, however, the p -wave interaction and the surface effects, disregarded in our calculation, have been taken into account; therefore the agreement shown in Fig. 9 has to be considered with some caution. It should be pointed out, in this regard, that our aim was mainly to illustrate the potentiality of the y -scaling analysis of the electromagnetic responses showing, e.g., that the q -behavior of F_L represents a serious test of various values of Landau-Migdal parameters, rather than to fit the experimental data. In this respect an analysis of F_L of the type presented in this paper, taking into account p -wave interaction and surface effects, would be highly necessary.

As far as the transverse channel is concerned, the central parameter is g' . Its value ranges in the literature from 0.5 to 0.8 (without excluding however other values). It is commonly believed at present that a value $g' \geq 0.6$ is required to prevent pion condensation and precursor phenomena, but since g' may depend on momentum and energy,^{38,39} the use of such a constraint in the quasielastic region is not a stringent one. The relevant point here is that the interaction is repulsive for small q where g' dominates, but the weight of the ρ exchange (which is attractive) increases with q . With $g'=0.5$ and $y=0$, for instance, the effective interaction changes sign at $q \approx 400$ MeV/c.

The effect of the Δ -hole is also relevant. An order-of-magnitude estimate for $y=0$ provides

$$\Pi_{\Delta h} \simeq \frac{16}{9} \frac{\rho}{(M_{\Delta} - M)}, \quad (54)$$

which has the same sign of Π^{adv} and at $q=400$ MeV/c holds about a 60% of Π^{adv} . At higher momenta where the interaction is always attractive its relative weight is further increasing.

In Fig. 10 the transverse scaling function for ^{40}Ca is reported for different reasonable values of g' . It can be seen that unlike F_L (cf. Fig. 9) the HF limit (and therefore the scaling) is not recovered, particularly at $y=0$, and that different values of g' seem to lead to an almost constant shift of F_T .

To sum up, the following comments concerning the results presented in this section are in order as follows.

(1) The connection of the scaling function with nuclear dynamics has been put in evidence. As shown in the figures of this section, by plotting the q dependence of F_L and F_T for fixed values of y the analysis of the inclusive q.e. data is remarkably improved.

(2) The effect of the q dependence of the effective interaction has been clearly outlined. For instance the q dependence of Ref. 8 changes drastically the shape of the curve.

(3) At low q , the disagreement with experimental data increases with increasing values of y . This is a clear manifestation of the relevance of the surface effects and it points to the potentiality of our analysis in establishing

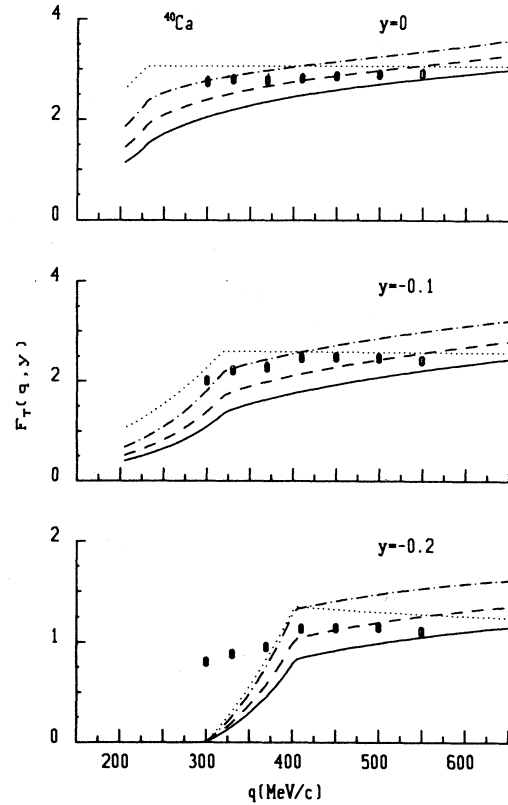


FIG. 10. Transverse scaling function for ^{40}Ca for different values of g' (ρ exchange and Δ -h contributions are included). Scaling variable and experimental data as in Fig. 7. Dash-dotted lines correspond to $g'=0.4$, dashed lines to $g'=0.6$, and dotted lines to $g'=0.8$. The solid lines represent pure Hartree-Fock approximation.

the limits of validity of a "Fermi-gas" model for inclusive scattering.

(4) Whereas F_L^{th} seems to approach an asymptotic value with increasing q , F_T^{th} on the contrary exhibits an appreciable increase with q , which is mainly due to the Δ -h intermediate states. It is clear that the future measurements at higher values of y will represent a severe test of effective nucleon-nucleon effective forces within the context of the application of many-body approaches for infinite systems to finite nuclei.

V. CONCLUSIONS

In this paper the concept of y scaling has been used to systematically investigate longitudinal and transverse responses. Our analysis of q.e. responses in terms of their q and y dependences had the following advantages with respect to the usual analysis in terms of their q and ω dependence: The plot versus q of various sets of data, corresponding to different kinematics but to the same value of y , had provided us with the experimental q dependence of those effects which break down the impulse approximation and the simple Hartree-Fock approximation; since different kinds of contributions to the q.e. cross sections are singled out for different values of y

($y \sim 0$, scattering from quasifree nucleons; $y > k_F$, surface effects; $y \gg k_F$, scattering from correlated nucleons, etc.), plotting the q dependence of $F_{L(T)}(q, y)$ for various values of y yields unique information on many-particle effects in different regimes of nucleon dynamics. The main conclusions which should be drawn from our analysis can be summarized as follows.

(1) The usual treatment of FSI within the impulse approximation, using optical potentials which contain a minimum of state dependence through the values of the single-particle energies [cf, Eqs. (28)–(31)], provides a reasonable description of the longitudinal response but is unable to generate any splitting between F_L and F_T . Several effects have been left out in the approach presented in Sec. III, namely those related to the necessary improvements of the DWIA and those related to the meson exchange currents (MEC) in the transverse channel. Since the latter ones are expected to be of minor relevance at large values of y , (i.e., for $\omega < \omega_{\text{peak}} = q^2/2M$), where the relative splitting is roughly of the same order as that at $y = 0$, the effect of the MEC cannot be considered as the main origin of the splitting. The results of the many-body approach presented in Sec. IV clearly show that the failure of the DWIA in generating the splitting is essentially due to the product form of the final state both in the longitudinal and transverse chan-

nels. Therefore future efforts should be focused on the construction of a final state allowing for a state dependent correlation between the emitted nucleus and the residual system.

(2) The splitting between the two channels induced by the effective interaction goes into the right direction, but clearly something is missing. The drawbacks of our model are of course the lack or too crude a parametrization of the q and ω dependences of effective masses, self-energies and effective interactions as well as the complete neglecting of any imaginary part for these quantities. Both these effects may come from a more complicated diagram involving light mesons (pions) and other particle-hole pairs, as those arising in the analysis presented in Ref. 31; however, such an analysis has been carried out at fixed momentum transfer, while it would be of great interest to repeat calculations for fixed y . It is clear however that a rich many-body calculation seems to be necessary in order to microscopically explain the splitting between F_L and F_T .

(3) Present data do not allow us to make any expectation about the behavior of the splitting at higher values of y . Such a behavior on the other hand would represent a decisive test to confirm or rule out different models of the reaction mechanisms and/or the residual N - N interaction.

- ¹B. P. Quinn *et al.*, Phys. Rev. C **37**, 1609 (1988).
- ²C. Marchand *et al.*, Phys. Lett. **153B**, 29 (1985); K. Dow, Ph.D. thesis, MIT, 1987.
- ³P. Barreau *et al.*, Nucl. Phys. **A402**, 515 (1983).
- ⁴Z. E. Meziani *et al.*, Phys. Rev. Lett. **52**, 2180 (1984); **54**, 1233 (1985).
- ⁵C. C. Blatchey *et al.*, Phys. Rev. C **34**, 1243 (1986).
- ⁶J. V. Noble, Phys. Rev. Lett. **46**, 12 (1981).
- ⁷L. S. Celenza, A. Harindranath, A. Rosenthal, and C. M. Shakin, Phys. Rev. C **31**, 946 (1985); P. J. Mulders, Nucl. Phys. **A459**, 525 (1986).
- ⁸W. M. Alberico, P. Czerski, M. Ericson, and A. Molinari, Nucl. Phys. **A462**, 269 (1987).
- ⁹S. Fantoni and V. R. Pandharipande, Nucl. Phys. **A473**, 134 (1987).
- ¹⁰M. Cavinato *et al.*, Nucl. Phys. **A423**, 376 (1984).
- ¹¹A. Dellafiore, F. Lenz, and F. A. Brieva, Phys. Rev. C **31**, 1088 (1985).
- ¹²S. Drozd, G. Cò, J. Wambach, and J. S. Speth, Phys. Lett. B **185**, 287 (1987).
- ¹³U. Stroth, R. Hasse, and P. Schuck, Nucl. Phys. **A462**, 45 (1987).
- ¹⁴I. Sick, D. Day, and J. S. McCarthy, Phys. Lett. **45**, 871 (1980).
- ¹⁵P. Bosted *et al.*, Phys. Rev. Lett. **49**, 1380 (1982); D. Day *et al.*, *ibid.* **39**, 472 (1987).
- ¹⁶C. Ciofi degli Atti, Progr. Part. Nucl. Phys. **3**, 163 (1980).
- ¹⁷L. Fetter and J. D. Walecka, *Quantum Theory of Many-Particle Systems* (McGraw-Hill, New York, 1971).
- ¹⁸G. B. West, Phys. Rep. **18**, 263 (1975).
- ¹⁹C. Ciofi degli Atti, E. Pace and G. Salmè, Phys. Lett. **127B**, 303 (1983); Few Body Systems, Suppl. **1**, 280 (1986).
- ²⁰C. Ciofi degli Atti, Nuovo Cimento Lett. **41**, 161 (1984).
- ²¹S. A. Gurvitz, J. A. Tjon, and S. J. Wallace, Phys. Rev. C **34**, 648 (1986).
- ²²S. A. Gurvitz and A. S. Rinat, Phys. Rev. C **35**, 696 (1987).
- ²³J. M. Finn, R. W. Lourie and B. H. Cottmann, Phys. Rev. C **29**, 2230 (1984).
- ²⁴C. Ciofi degli Atti and G. Salmè, Proceedings of the 6th Seminar on Electromagnetic Interactions of Nuclei at Low and Medium Energies, Moscow, 1984, edited by L. E. Larareva (Academy of Sciences USSR, Moscow, 1985), p. 224.
- ²⁵E. Pace and G. Salmè, Phys. Lett. **110B**, 411 (1982).
- ²⁶O. Benhar, E. Pace and G. Salmè, Phys. Lett. B **195**, 13 (1987).
- ²⁷T. de Forest, Nucl. Phys. **A392**, 411 (1982).
- ²⁸M. Gari and K. Kruempelman, Phys. Lett. B **177**, 90 (1986).
- ²⁹T. De Forest, Nucl. Phys. **A132**, 305 (1969).
- ³⁰H. Orland and R. Schaeffer, Nucl. Phys. **A299**, 442 (1978).
- ³¹W. M. Alberico, M. Ericson, and A. Molinari, Ann. of Phys. **154**, 356 (1984).
- ³²J. M. Laget, Phys. Lett. **151B**, 325 (1985).
- ³³See for instance G. E. Brown, *Unified Theory of Nuclear Models and Forces* (North Holland, Amsterdam 1971).
- ³⁴G. Höler and E. Pietarinen, Nucl. Phys. **B95**, 210 (1975).
- ³⁵E. J. Moniz, Phys. Rev. **184**, 1155 (1969).
- ³⁶J. Speth, E. Werner, and W. Wild, Phys. Rep. **33C**, 127 (1976).
- ³⁷W. M. Alberico, R. Cenni, M. B. Johnson, and A. Molinari, Ann. of Phys. **138**, 178 (1982).
- ³⁸W. H. Dickhoff, A. Faessler, J. Meyer-ter-Vehn and H. Mütter, Phys. Rev. C **23**, 1154 (1981); Nucl. Phys. **A368**, 445 (1981).
- ³⁹R. Cenni, G. Dillon, and P. Saracco, Nuovo Cimento **A77**, 231 (1983).